

P₄ Activation

International Edition: DOI: 10.1002/anie.201510716

German Edition: DOI: 10.1002/ange.201510716

Influence of the nacnac Ligand in Iron(I)-Mediated P₄ Transformations

Fabian Spitzer, Christian Graßl, Gábor Balázs, Eva M. Zolnhofer, Karsten Meyer, and Manfred Scheer*

Dedicated to Professor Hangeorg Schnöckel on the occasion of his 75th birthday

Abstract: A study of P₄ transformations at low-valent iron is presented using β-diketiminato (L) Fe^I complexes [LFe(tol)] (tol = toluene; L = L¹ (**1a**), L² (**1b**), L³ (**1c**)) with different combinations of aromatic and backbone substituents at the ligand. The products [(LFe)₄(μ₄-η²:η²:η²:η²-P₈)] (L = L¹ (**2a**), L² (**2b**)) containing a P₈ core were obtained by the reaction of **1a,b** with P₄ in toluene at room temperature. Using a slightly more sterically encumbered ligand in **1c** results in the formation of [(L³Fe)₂(μ-η⁴:η⁴-P₄)] (**2c**), possessing a cyclo-P₄ moiety. Compounds **2a–c** were comprehensively characterized and their electronic structures investigated by SQUID magnetization and ⁵⁷Fe Mössbauer spectroscopy as well as by DFT methods.

The activation of white phosphorus (P₄) with main-group^[1] and transition-metal^[2] compounds is an ongoing area of research. The latter topic is dominated by Cp^R containing transition-metal complexes.^[2] More recently, complexes of the β-diketiminato (nacnac = L) ligand have been employed for P₄ activation as well. For early transition-metal compounds, exclusively Group 5 complexes were used,^[3] whereas for electron-rich metals Group 8–10 complexes have been applied so far.^[4] Selected examples of P_n complexes **A–D** with β-diketiminato ligands of late transition metals are shown in Figure 1. Recently, we reported on the Cu^I compounds [(LCu)₂(μ-η²:η²-E₄)] (E = P (**D**), As) and [LCu(η²-P₄)], respectively, containing intact E₄ moieties,^[5] while all other examples (**A–C**) contain transformed P₄ units. Also, we investigated the reaction of Fe^I complexes [LFe(tol)] with P₄. When the Driess group recently reported on the formation of

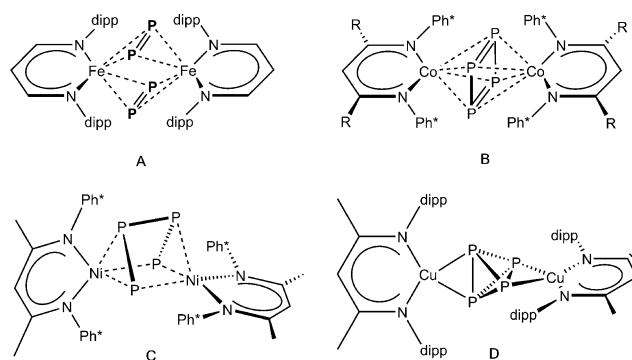


Figure 1. Selected examples of P_n complexes with late transition metals Fe, Co, Ni, and Cu supported by the β-diketiminato ligand.^[4,5]

the Fe^{III} complex [(L⁰Fe)₂(μ-η²:η²-P₂)₂] (**A**), containing two dianionic P₂ ligands,^[4a] we were surprised as our investigations showed quite different results. Since the reaction conditions were identical, we supposed that the reason for the different P₄ activation pathways (and products) was due to the slightly different aromatic flanking groups and α-backbone substituents of our [LFe(tol)] precursors. Therefore, we systematically studied the driving forces for the different outcome of P₄ activation by Fe^I centers.

Herein, we present a comparative study of P₄ activation by Fe^I β-diketiminato (L) complexes [LFe(tol)] (L = L¹ (**1a**), L² (**1b**), L³ (**1c**)) with toluene (tol) as a labile leaving group. The starting materials [LFe(tol)] (L = L¹ (**1a**), L² (**1b**), L³ (**1c**)) were synthesized in a one-pot synthesis (see the Supporting Information) and characterized by single-crystal X-ray crystallography (**1b** and **1c**, see the Supporting Information).

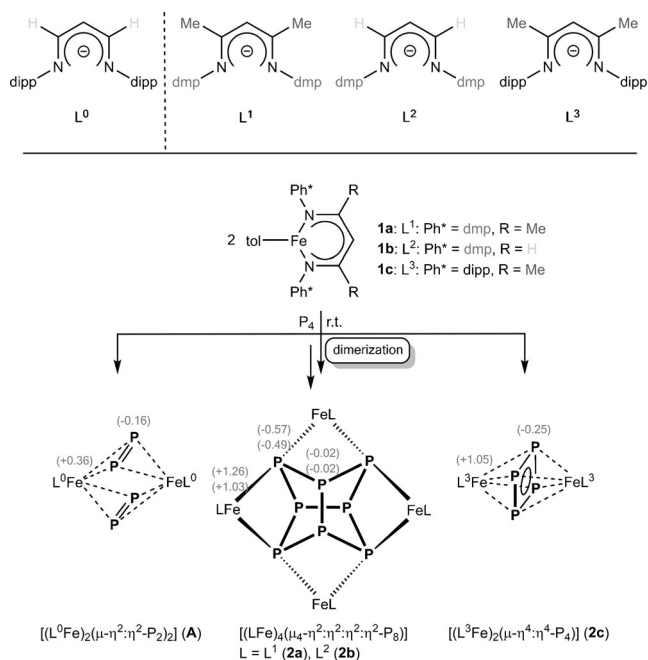
The reaction of [L¹Fe(tol)] (**1a**) with 0.5 equivalent of P₄ in toluene at room temperature leads to the formation of a tetranuclear complex, namely [(L¹Fe)₄(μ₄-η²:η²:η²:η²-P₈)] (**2a**), which displays a realgar-type^[6] P₈ moiety. Changing the stoichiometry of the reaction does not affect the product formation (ratio [L¹Fe(tol)]/P₄ = 2:1 and 1:2). The formation of a P₈ moiety in **2a** is in contrast to the recently reported product, [(L⁰Fe)₂(μ-η²:η²-P₂)₂] (**A**), published by the Driess group,^[4a] which contains two [P₂]²⁻ ligands (Scheme 1). A comparison of ligand L⁰ with L¹, however, displays only small differences in the aromatic (Ph* = dipp (= 2,6-diisopropylphenyl) or dmp (= 2,6-dimethylphenyl)) and in the backbone (R) substituents. In both cases the reaction conditions were identical. Therefore, we were interested to understand whether the steric demand or the electronic properties of the aromatic flanking groups Ph* and backbone α-substitu-

[*] M. Sc. F. Spitzer, Dr. C. Graßl, Dr. G. Balázs, Prof. Dr. M. Scheer
Institut für Anorganische Chemie, Universität Regensburg
Universitätsstrasse 31, 93040 Regensburg (Germany)
E-mail: manfred.scheer@chemie.uni-regensburg.de
Homepage: <http://www.uni-regensburg.de/chemie-pharmazie/anorganische-chemie-scheer/>

M. Sc. E. M. Zolnhofer, Prof. Dr. K. Meyer
Friedrich-Alexander University Erlangen-Nürnberg (FAU)
Department of Chemistry and Pharmacy, Inorganic Chemistry
Egerlandstrasse 1, 91058 Erlangen (Germany)

Supporting information for this article can be found under <http://dx.doi.org/10.1002/anie.201510716>.

© 2016 The Authors. Published by Wiley-VCH Verlag GmbH & Co. KGaA. This is an open access article under the terms of the Creative Commons Attribution Non-Commercial NoDerivs License, which permits use and distribution in any medium, provided the original work is properly cited, the use is non-commercial and no modifications or adaptations are made.



Scheme 1. Top: Comparison of L^0 with ligands L^1 , L^2 , and L^3 , containing a variety of different substituents. Bottom: Coordinated P_n moieties obtained by P_4 transformation with different Fe^I precursors. The gray numbers in brackets represent the NPA charges at the corresponding atoms.^[7] For **2a, b** the upper value corresponds to **2a**.

ents R cause the different reactivity of the Fe^I precursors towards P_4 . According to DFT calculations at the BP86//def2-SVP/def2-TZVP (N, Fe, P) level, the dimerization of the hypothetical complex $[(L^I Fe)_2(\mu-\eta^4-\eta^4-P_4)]$ (quintet spin state) to **2a** (nonet spin state) is endothermic (91.5 kJ mol^{-1}). This seems to be in contrast with the experimental results. However, considering that the unrestricted singlet spin state of **2a** is more stable than the nonet spin state ($102.1 \text{ kJ mol}^{-1}$), the reaction becomes exothermic. Furthermore, the natural population analyses (NPA) clearly indicates the presence of Fe^{II} centers and $[P_8]^{4-}$ ligand in **2a**.

Accordingly, we decided to additionally synthesize ligand L^2 (see Scheme 1, top), representing the missing combination between ligands L^0 and L^1 , to investigate the steric and electronic effects induced by the different substitution of the chelating N atoms and the ligand backbone. Conducting the reaction of $[L^2Fe(tol)]$ (**1b**) and P_4 under identical conditions (RT, toluene) and same stoichiometries (2:1 and 1:2) facilitates the clean and selective formation of the P_8 moiety containing complex $[(L^2Fe)_4(\mu_4-\eta^2-\eta^2-\eta^2-\eta^2-P_8)]$ (**2b**) (Figure 2). Even if a higher local concentration of P_4 was used by the dropwise addition of 1 equivalent of **1b** to a solution of 2 equiv of P_4 in toluene, **2b** is the only product of the reaction. Comparing **2a** and **2b**, we assume that the methyl flanking groups in dmp are not able to prevent the dimerization reaction to the P_8 moiety, as the dipp substituents did in $[(L^0Fe)_2(\mu-\eta^2-\eta^2-P_2)_2]$ (**A**). Along with **A**,^[4a] possessing two separate P_2 units, compounds **2a, b** are different activation steps of P_4 (Scheme 1).

A single-crystal X-ray structural analysis reveals that compounds **2a**·2toluene and **2b**·toluene are isostructural

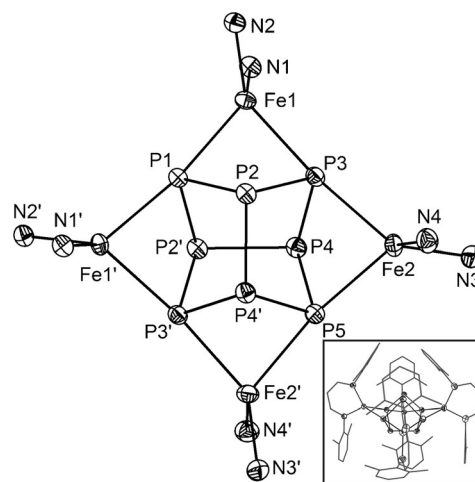


Figure 2. Core structure of **2b** in crystals of **2b**·toluene (hydrogen and carbon atoms are omitted for clarity; ellipsoids are set at 50% probability).^[15] A representation of **2b** with its complete ligands is shown in the inset.

(Figure 2 for **2b**). Both compounds contain a realgar-type P_8 ligand coordinating to four $[L^I Fe]$ ($L = L^1$ (**2a**), $L = L^2$ (**2b**)) fragments. All P–P distances are in the range of 2.1991(8) to 2.2813(7) Å in **2a** and 2.2111(6) to 2.2792(6) Å in **2b**; and therefore, are in line with P–P single bonds (for comparison: P–P single bond in white phosphorus determined by electron diffraction: 2.1994(3) Å,^[8] Raman spectroscopy: 2.2228(5) Å,^[9] and DFT calculations: 2.1994(3) Å^[8]). The coordination geometry of the Fe metal centers in **2a** and **2b**, respectively, is best described as distorted tetrahedral. The torsion angles between the Fe–P–P and Fe–N–N planes are between 74.66(6)° and 84.74(5)° in **2a** and 83.45(4)° and 84.91(6)° in **2b**. There are no significant differences in the P–P bond distances in **2a, b** and those of previously reported related P_8 ligands in $[(NN^{tC}Sc)_4P_8]$, $[(Cp^*Sm)_4P_8]$ ($Cp^* = C_5Me_5$), $[Cp^{Me}Fe_4(CO)_6P_8]$ ($Cp^{Me} = C_5H_4Me$), $[(Cp^{Me}Fe_4(CO)_{13}P_8)]$, and $[Cp^*Ir_2Cr_3(CO)_{17}P_8]$.^[10]

The Fe–N distances lie between 1.983(2) and 2.006(2) Å in **2a** and between 1.982(2) and 1.990(2) Å in **2b**. The distances of Fe and the coordinating phosphorus atoms are in the range of 2.4559(6) and 2.5006(6) Å in **2a** and 2.4583(3) and 2.4807(5) Å in **2b**, respectively.

No signals were detected in the $^{31}P\{^1H\}$ NMR spectra of **2a, b**. These solutions (**2a** in C_6D_6 and **2b** in $[D_8]toluene$) are also EPR-silent at RT as well as at 10 K, suggesting a higher spin multiplicity or antiferromagnetically coupled iron centers that result in a non-magnetic (EPR-silent) ground state at low temperature. However, the 1H NMR spectra of **2a** and **2b** reveal signals in the range from 273 ppm to –29 ppm; thus indicating a paramagnetic spin state for **2a, b**. The careful analysis of the spectra enabled us to assign all resonances (see the Supporting Information). The effective magnetic moment (μ_{eff}) at room temperature was determined to be 6.79 μ_B for **2a** in C_6D_6 and 6.71 μ_B for **2b** in $[D_8]THF$ solution (Evans method). These values are well-confirmed by temperature-dependent SQUID measurements in the solid state. Both complexes exhibit a similar magnetic behavior with a strong

temperature dependency of their effective magnetic moments over a temperature range between 2 and 300 K. At 2 K, the effective magnetic moments amount to $1.14 \mu_{\text{B}}$ (**2a**) and $0.54 \mu_{\text{B}}$ (**2b**). With increasing temperature, the magnetic moments gradually increase until effective magnetic moments of $7.04 \mu_{\text{B}}$ (**2a**) and $6.92 \mu_{\text{B}}$ (**2b**) are reached at 300 K (see the Supporting Information). This magnetic behavior is likely caused by an antiferromagnetic coupling. The zero-field ^{57}Fe Mössbauer spectrum of **2b** at 77 K shows a doublet with an isomer shift δ of $0.73(1) \text{ mms}^{-1}$ and a quadrupole splitting ΔE_{Q} of $1.93(1) \text{ mms}^{-1}$, which is in agreement with a high-spin iron(II) complex. Similar Mössbauer parameters have been observed in the four-coordinate iron(II) complex $[\text{PhB}(\text{MesIm})_3\text{Fe}(\text{N}=\text{PPh}_3)]$.^[11] The presence of iron(II) centers in **2b** is also indicated by NPA analysis.

So far, we assume that the aromatic dmp substituents at the coordinating N atoms of the ligand play a crucial role for the formation of the P_8 ligand moieties in **2a** and **2b**, and the α -substituent of the ligand backbone does not have much influence on the outcome of P_4 activation. Regardless, to conclusively address this point, the ligand L^3H was synthesized (Scheme 1). While L^3 features aromatic dipp groups at the coordinating N atoms (like L^0), its ligand backbone is substituted with two Me α -substituents (like L^1); and hence, represents the missing hybrid ligand between L^0 and L^1 . Owing to steric reasons, the Me substituents at the ligand backbone are restricting the rotational flexibility of the P groups in dipp, thus increasing their steric pressure.^[12]

The reaction of **1c** with 0.5 equivalent of P_4 in toluene at RT leads to the formation of $[(\text{L}^3\text{Fe})_2(\mu\text{-}\eta^4\text{:}\eta^4\text{-P}_4)]$ (**2c**), containing a *cyclo*- P_4 moiety. Again, changing the stoichiometry of the reaction does not have an effect on the product formation ($[(\text{L}^3\text{Fe}(\text{tol})]/\text{P}_4 = 2:1$ and $1:2$). Different from our experience with the complexes of the dmp containing ligands L^1 and L^2 , we now obtain a *cyclo*- P_4 unit in the product **2c**, which is also in contrast to Driess' product **A**, featuring two separated P_2 units (Scheme 1).

Single crystals of **2c** suitable for X-ray diffraction were grown from a saturated toluene solution (Figure 3). Compound **2c** is a centrosymmetric dinuclear iron complex that consists of two $[\text{L}^3\text{Fe}]$ fragments bridged by a planar *cyclo*- P_4 ligand. The middle deck displays weak disorder (occupancy 97:3; see the Supporting Information). In the following, only the major component of the middle deck is discussed. The $\text{P}-\text{P}$ distances within the central P_4 moiety ($\text{P1}-\text{P2}$ and $\text{P1}-\text{P2}'$) in **2c** amount to $2.178(1)$ and $2.207(1) \text{ \AA}$, respectively. These distances are longer than those reported for *cyclo*- $[\text{P}_4]^{2-}$ ligands ($2.146(1)$ – $2.1484(9) \text{ \AA}$)^[13] and shorter than those reported for *cyclo*- $[\text{P}_4]^{4-}$ moieties ($2.230(2)$ – $2.259(2) \text{ \AA}$).^[14] The angles of $\text{P2}'-\text{P1}-\text{P2}$ and $\text{P1}-\text{P2}-\text{P1}'$ are $91.73(3)^\circ$ and $88.27(3)^\circ$, respectively, indicating a slightly distorted ring conformation. The $\text{Fe}-\text{P}$ distances are between $2.4376(6)$ and $2.5163(6) \text{ \AA}$, comparable to those observed in **2a** and **2b**. Similarly, the $\text{Fe}-\text{N}$ distances in **2c** ($2.018(2)$ and $2.025(2) \text{ \AA}$) are comparable to **A** ($2.023(3)$ and $2.025(3) \text{ \AA}$),^[14a] but slightly elongated compared to **2a** ($1.983(2)$ and $2.006(2) \text{ \AA}$) and **2b** ($1.982(2)$ and $1.990(2) \text{ \AA}$). The $\text{Fe1}-\text{Fe1}'$ distance in **2c** is 3.902 \AA , being significantly elongated compared to compound **A** (2.777 \AA). One of the most remarkable differences between

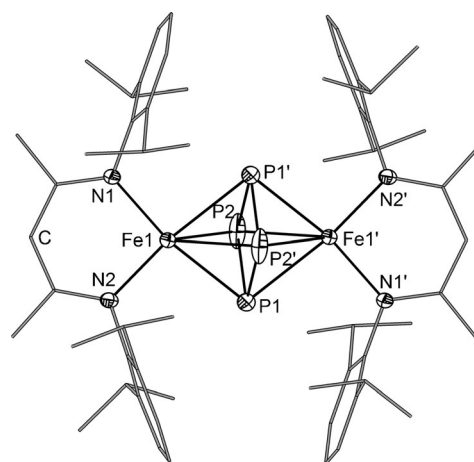


Figure 3. Molecular structure of **2c** (hydrogen atoms are omitted for clarity; ellipsoids are set at 50% probability).^[15] Selected bond lengths [\AA] and angles [$^\circ$]: $\text{P1}-\text{P2}$ $2.178(1)$, $\text{P1}-\text{P2}'$ $2.207(1)$, $\text{Fe1}-\text{P1}$ $2.4376(6)$, $\text{Fe1}-\text{P2}$ $2.5064(6)$, $\text{Fe1}-\text{P1}'$ $2.5163(6)$, $\text{Fe1}-\text{P2}'$ $2.5064(6)$, $\text{Fe1}-\text{N1}$ $2.018(2)$, $\text{Fe1}-\text{N2}$ $2.025(2)$, $\text{Fe1}-\text{Fe1}'$ 3.902 ; $\text{P2}'-\text{P1}-\text{P2}$ $91.73(3)$, $\text{P1}-\text{P2}-\text{P1}'$ $88.27(3)$.

2c and **A** is the torsion angle θ between the $\text{Fe}-\text{Fe}$ axis and the plane formed by the nitrogen atoms and the methine carbon atom in the ligand backbone, which is considerably smaller in **2c** (15°) compared to **A** (33° ; Figure 4).

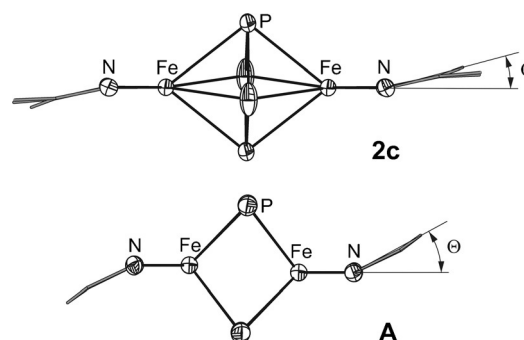


Figure 4. Comparison of the coordination geometry in **2c** and **A**.^[14a]

Like in the tetranuclear complexes **2a,b**, no resonances were detected in the $^{31}\text{P}\{^1\text{H}\}$ NMR spectra of **2c** and solutions of **2c** are EPR-silent at room temperature and at 10 K. However, the ^1H NMR spectra of **2c** in $[\text{D}_8]\text{THF}$ reveals signals in the range from 7 ppm to -2 ppm. The magnetic moment of **2c** in $[\text{D}_8]\text{THF}$ at RT was determined to be $3.09 \mu_{\text{B}}$ (Evans method). Temperature-dependent SQUID measurements in the solid state are in agreement with this result with an effective magnetic moment of $3.46 \mu_{\text{B}}$ at 300 K. The magnetism of complex **2c** is strongly temperature-dependent. At 2 K, the effective magnetic moment was determined to be $0.54 \mu_{\text{B}}$, and is rising to $1.00 \mu_{\text{B}}$ at 20 K. Between 20 and 80 K, it remains roughly constant. Increasing the temperature to 300 K leads to a gradual increase of the effective magnetic moment up to a value of $3.46 \mu_{\text{B}}$ at 300 K (see the Supporting Information). This magnetic behavior is explained by a $S_{\text{tot}} =$

0 ground state between 0 and 80 K and antiferromagnetic coupling of the two iron nuclei at higher temperatures. The zero-field ^{57}Fe Mössbauer spectrum of **2c** at 77 K features a doublet with an isomer shift δ of 0.74(1) mms^{-1} and a quadrupole splitting ΔE_{Q} of 1.74(1) mms^{-1} , which is very similar to the Mössbauer parameters of **2b** and is in accordance with a high-spin iron(II) complex.

The optimized geometry of **2c** in the quintet spin state obtained from DFT calculations (BPW91/def2-SVP) is in good agreement with the experimentally found geometric parameters, with a slightly shorter Fe–Fe distance (3.827 Å) and slightly longer P–P distances (2.203–2.250 Å).^[15] Notably, the geometry optimization in the unrestricted singlet spin state instead leads to further shortening of the Fe–Fe distance (3.712 Å) and to a planar P_4 ring with two shorter and two longer P–P distances (2.181 Å and 2.325 Å, respectively). Since the Fe–Fe distance in **A** (2.777 Å) is significantly shorter than in **2c**, the geometry of **2c** (quintet spin state) was optimized with a fixed Fe–Fe distance of 2.777 Å. In the optimized geometry, the *cyclo*- P_4 unit is cleaved into two P_2 units and the nacnac ligand shows the same type of folding like the one reported for **A**. The energy difference between both isomers is 29.19 kJ mol^{-1} , favoring the relaxed geometry of **2c**. This points towards a flat energy surface and suggests that the outcome of the P_4 transformation is mostly determined by the Fe–Fe distance. Broken symmetry calculations (BPW91//def2-SVP/aug-cc-pVTZ (Fe, P)) indicate an antiferromagnetic coupling between the two Fe centers, which increases with the decrease of the Fe–Fe distance.^[15] The Mulliken population analysis for the quintet spin state of **2c** shows that the spin density is localized on iron atoms, but no considerable spin density was found on the P_4 or nacnac ligands. The Mayer bond order for the P–P bonds vary from 0.81 to 0.87; thus, indicating P–P single bonds.

In conclusion, we have shown that the different reactivity of β -diketiminato Fe^{I} complexes $[\text{LFe}(\text{tol})]$ ($\text{L} = \text{L}^1$ (**1a**), L^2 (**1b**), L^3 (**1c**)) towards P_4 is sensitive to minimal changes in the ligand: its flanking groups (Ph^*) and its backbone α -substituents (R). By conducting the reactions under similar conditions (RT) in the same solvent (toluene), and using exact stoichiometric amounts of P_4 ($[\text{LFe}(\text{tol})]/\text{P}_4 = 2:1$) or even larger amounts of P_4 ($[\text{LFe}(\text{tol})]/\text{P}_4 = 1:2$), a different outcome of P_4 activation is realized. By employing the aromatic dmp flanking groups as substituents of the coordinating N atoms, the formation of a $[\text{P}_8]^{4-}$ structural motif in the iron(II) compounds $[(\text{LFe})_4(\mu_4\text{-}\eta^2\text{-}\eta^2\text{-}\eta^2\text{-}\eta^2\text{-}\text{P}_8)]$ ($\text{L} = \text{L}^1$ (**2a**), $\text{L} = \text{L}^2$ (**2b**)) is observed.^[17b] Employing the sterically more demanding dipp substituents leads to the formation of an iron(II) compound $[(\text{L}^3\text{Fe})_2(\mu\text{-}\eta^4\text{-}\eta^4\text{-}\text{P}_4)]$ (**2c**), containing a *cyclo*- $[\text{P}_4]^{2-}$ moiety. This finding is in contrast to the formation of two separate $[\text{P}_2]^{2-}$ units observed in the iron(III) complex **A**, with two H α -substituents being located in the ligand backbone instead of Me atoms in **2c**. This demonstrates the additional steric influence of the Me groups as α -substituents to push the dipp substituents closer together, thereby preventing the opening of the *cyclo*- P_4 ring by relaxing the Fe...Fe distance in **2c** in comparison with the rather short distance in **A**. The discussed ligand dependencies in the β -diketiminato ligand complexes may foster the systematic study of such depend-

encies in other metal systems for the activation of small molecules in general and in particular for the controlled P_n ligand formation from white phosphorus.

Acknowledgments

This work was supported by the Deutsche Forschungsgemeinschaft. The European Research Council (ERC) is acknowledged for the support in the SELFPHOS AdG-339072 project.

Keywords: Mössbauer spectroscopy · paramagnetic compounds · small-molecule activation · substituent effects · white phosphorus

How to cite: *Angew. Chem. Int. Ed.* **2016**, *55*, 4340–4344
Angew. Chem. **2016**, *128*, 4412–4416

- [1] a) M. Scheer, G. Balázs, A. Seitz, *Chem. Rev.* **2010**, *110*, 4236–4256; b) S. Khan, S. S. Sen, H. W. Roesky, *Chem. Commun.* **2012**, 48, 2169–2179; c) N. A. Giffin, J. D. Masuda, *Coord. Chem. Rev.* **2011**, 255, 1342–1359.
- [2] a) B. M. Cossairt, N. A. Piro, C. C. Cummins, *Chem. Rev.* **2010**, *110*, 4164–4177; b) M. Caporali, L. Gonsalvi, A. Rossin, M. Peruzzini, *Chem. Rev.* **2010**, *110*, 4178–4235.
- [3] a) B. L. Tran, M. Singhal, H. Park, O. P. Lam, M. Pink, J. Krzystek, A. Ozarowski, J. Telser, K. Meyer, D. J. Mindiola, *Angew. Chem. Int. Ed.* **2010**, *49*, 9871–9875; *Angew. Chem.* **2010**, *122*, 10067–10071; b) C. Camp, L. Maron, R. G. Bergman, J. Arnold, *J. Am. Chem. Soc.* **2014**, *136*, 17652–17661; c) B. Pintér, K. T. Smith, M. Kamitani, E. M. Zolnhofer, B. L. Tran, S. Fortier, M. Pink, G. Wu, B. C. Manor, K. Meyer, M.-H. Baik, D. J. Mindiola, *J. Am. Chem. Soc.* **2015**, *137*, 15247–15261.
- [4] a) S. Yao, T. Szilvasi, N. Lindenmaier, Y. Xiong, S. Inoue, M. Adelhardt, J. Sutter, K. Meyer, M. Driess, *Chem. Commun.* **2015**, 51, 6153–6156; b) S. Yao, N. Lindenmaier, Y. Xiong, S. Inoue, T. Szilvasi, M. Adelhardt, J. Sutter, K. Meyer, M. Driess, *Angew. Chem.* **2015**, *127*, 1266–1270; c) S. Yao, Y. Xiong, C. Milsmann, E. Bill, S. Pfirrmann, C. Limberg, M. Driess, *Chem. Eur. J.* **2010**, *16*, 436–439.
- [5] F. Spitzer, M. Sierka, M. Latronico, P. Mastrorilli, A. V. Virovets, M. Scheer, *Angew. Chem. Int. Ed.* **2015**, *54*, 4392–4396; *Angew. Chem.* **2015**, *127*, 4467–4472.
- [6] The term “realgar-type” P_8 moiety for the tricyclo[3.3.0.0^{3,7}]octaphosphane ligand comes from its analogy to the isostructural realgar (As_4S_4) molecule.
- [7] a) For **2a,b,c** calculated at the BP86/def2-SVP level. The NPA charges for **A** were taken from Ref. [4a]. It should be noted that different basis sets were used; b) For the relationship of the formal oxidation states and the spectroscopic and structural parameters (see the Supporting Information, Table S3).
- [8] B. M. Cossairt, C. C. Cummins, A. R. Head, D. L. Lichtenberger, R. J. F. Berger, S. A. Hayes, N. W. Mitzel, G. Wu, *J. Am. Chem. Soc.* **2010**, *132*, 8459–8465.
- [9] N. J. Brassington, H. G. M. Edwards, D. A. Long, *J. Raman Spectrosc.* **1981**, *11*, 346–348.
- [10] a) S. N. Konchenko, N. A. Pushkarevsky, M. T. Gamer, R. Köppe, H. Schnöckel, P. W. Roesky, *J. Am. Chem. Soc.* **2009**, *131*, 5740–5741; b) W. Huang, P. L. Diaconescu, *Chem. Commun.* **2012**, 48, 2216–2218; c) M. E. Barr, B. R. Adams, R. R. Weller, L. F. Dahl, *J. Am. Chem. Soc.* **1991**, *113*, 3052–3060; d) M. Scheer, U. Becker, E. Matern, *Chem. Ber.* **1996**, *129*, 721–724; for structurally similar As_8 complexes, see: C. Schwarzmaier, A. Y. Timoshkin, G. Balázs, M. Scheer, *Angew.*

- Chem. Int. Ed.* **2014**, *53*, 9077–9081; *Angew. Chem.* **2014**, *126*, 9223–9227.
- [11] J. J. Scepaniak, T. D. Harris, C. S. Vogel, J. Sutter, K. Meyer, J. M. Smith, *J. Am. Chem. Soc.* **2011**, *133*, 3824–3827.
- [12] D. J. E. Spencer, A. M. Reynolds, P. L. Holland, B. A. Jazdzewski, C. Duboc-Toia, L. Le Pape, S. Yokota, Y. Tachi, S. Itoh, W. B. Tolman, *Inorg. Chem.* **2002**, *41*, 6307–6321.
- [13] F. Kraus, J. C. Aschenbrenner, N. Korber, *Angew. Chem. Int. Ed.* **2003**, *42*, 4030–4033; *Angew. Chem.* **2003**, *115*, 4162–4165.
- [14] A. Velian, C. C. Cummins, *Chem. Sci.* **2012**, *3*, 1003–1006.
- [15] See the Supporting Information.

Received: January 13, 2016

Published online: February 29, 2016
